THE JOURNAL OF PHYSICAL CHEMISTRY B

Article

pubs.acs.org/JPCB

Spectroscopic Investigation of the pH Controlled Inclusion of Doxycycline and Oxytetracycline Antibiotics in Cationic Micelles and Their Magnesium Driven Release

Alessio Cesaretti, Benedetta Carlotti, Pier Luigi Gentili, Catia Clementi, Raimondo Germani, and Fausto Elisei*

Department of Chemistry, Biology and Biotechnology and Centre of Excellence on Nanostructured Innovative Materials (CEMIN), University of Perugia, via Elce di Sotto 8, 06123 Perugia, Italy

Supporting Information

ABSTRACT: This work presents a steady-state and time-resolved UV−visible spectroscopic investigation of two antibiotics belonging to the family of tetracyclines (doxycycline and oxytetracycline) in the micellar medium provided by *p*-dodecyloxybenzyltrimethylammonium bromide (*p*DoTABr). The spectroscopic analysis has been performed in absorption and emission with femtosecond time resolution, and at pH 5.0 and 8.7 where doxycycline and oxytetracycline are present in their neutral-zwitterionic and monoanionic forms, respectively. The experimental data have been processed by sophisticated data mining methods such as global/target analysis and the maximum entropy method. The results unambiguously indicate that, when doxycycline and oxytetracycline are in their zwitterionic form, they are entrapped within the micelle, while when they are in their monoanionic form, they preferentially show a strong one-to-one interaction with the positively charged surfactant heads. Thus, the pH of the solution controls the inclusion of the investigated drugs into the micelle. When the drugs are entrapped inside the micelles, their spectroscopic and dynamical properties after photoexcitation change appreciably. Interestingly, the entrapped drugs are still able to strongly bind Mg^{2+} cations, crucial in determining the biological functioning of tetracyclines. The femtosecond resolved measurements reveal that the drugs are efficiently pulled out of the micelles by Mg^{2+}. In fact, magnesium−tetracycline complexes are detected in the aqueous phase. The present study suggests the potential promising use of ammonium surfactant micelles embedding doxycycline and oxytetracycline as "smart" drug delivery systems allowing their pH controlled inclusion and Mg^{2+} induced release.

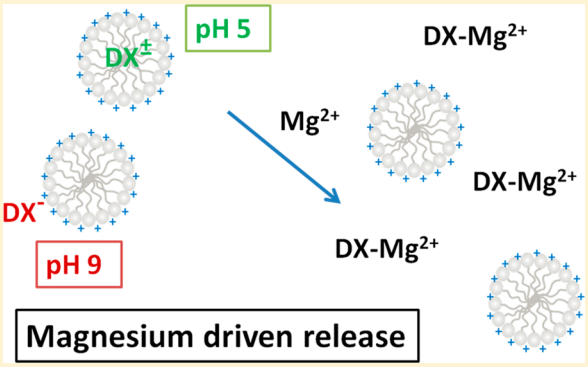

INTRODUCTION

Tetracyclines are an amazing class of drugs: they have been typically used as antibiotic agents, but they have now found novel multiple therapeutic potential.[1−3] Even though they have been first discovered in the 1950s, the increasing amount of published work and the number of ongoing clinical trials support the notion that there must be something unique about this family of organic compounds that still deserves attention. In fact, even merely from the chemical point of view, tetracyclines are molecules with an incredible richness of behavior. Their molecular structure is made of four fused rings (usually indicated as A, B, C, and D; see Chart 1) whose substituents in the lower peripheral region of the BCD portion and in the A moiety are fixed and characterize the entire class of compounds. On the other hand, the variable nature and position of the substituents placed in the upper peripheral region of the BCD moiety discriminate the several analogous components of the family conferring them surprisingly different properties. All tetracyclines show various acidic and basic sites (hydroxyl and amino groups) which may undergo deprotonation under different pH conditions.[4−8] This property confers them a wealthy acid−base chemistry. In fact, tetracyclines are characterized by at least three dissociation equilibria and they

Chart 1. Molecular Structures of the Investigated Tetracyclines

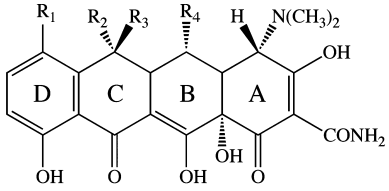

$R_1 = H; R_2 = CH_3; R_3 = H; R_4 = OH$ **(DX)**

$R_1 = H; R_2 = CH_3; R_3 = OH; R_4 = OH$ **(OX)**

Received: March 5, 2014
Revised: July 1, 2014
Published: July 1, 2014

exist in aqueous solution as differently protonated and therefore differently charged tetracyclines (cationic, zwitterionic, monoanionic, and bianionic species). Moreover, tetracyclines have been proven to show keto−enolic tautomerism involving the proximal ketonic and hydroxyl groups placed in the lower peripheral region of the BCD rings.[9−11] Still, they are conformationally flexible molecular systems,[10,12−14] and they have been, also, found to efficiently bind (in a 1:2 stoichiometry) biologically relevant metal cations, such as Mg^{2+}, Ca^{2+}, and Cu^{2+}, with the interaction strength and mechanism being strongly dependent upon the solution pH, the nature of the ion, and the structure of tetracycline.[15−17] For instance, among the six compounds investigated in our previous work,[18] doxycycline and oxytetracycline have exhibited different interaction sites for the cations between them and with respect to the parent tetracycline despite their very similar chemical structure. However, it has been generally observed that the spectral and photophysical properties of the Mg^{2+}−tetracycline complexes are strongly different from those of free drugs. Tetracycline has been recently investigated in confined environments, such as micellar and sol−gel media, and has been found to be able to distribute itself among the hydrophobic domains and the water pools that constitute the microheterogeneous sol−gel matrix.[19]

Self-assembled systems, sol−gel, and polymers draw an increasing attention because they could be used as efficient drug vehicles, particularly for compounds that are poorly soluble in water. Recently, there has been a strong incentive to develop drug delivery systems with smart functions such as target ability to specific tissues and chemical or physical stimuli sensitivity.[20−22] In particular, the smartness may lay in the ability to perceive the prevailing stimuli (pH, temperature, light, and salt concentration) and respond by exhibiting changes that result in the switchable inclusion or release of the entrapped drug. The capacity to respond to stimuli may be related to the host or to the guest; in the latter case, smart drug delivery systems may be obtained by employing chemically simple, not responsive surfactants. In the literature, there are several examples of polymeric micelles where the polymer−drug conjugate degrades depending on the pH (because of the hydrolytic breakage of a covalent bond), leading to a system where the drug release is controlled and occurs as needed in intracellular compartments (endosomes, lysosomes) where acidic pH conditions can be retrieved.[23−26]

Considering that the physical and chemical properties of tetracyclines can be modulated not only by their molecular structure but also by several external stimuli such as solution pH and presence of cations, it seems interesting to exploit their extreme responsiveness to develop smart delivery systems involving micelles as host. With the complexity and controllability being mainly associated with the drug itself, it appears feasible to use micelle aggregates that show simple interactions with the drug for this aim. Therefore, a comprehensive UV−visible spectroscopic investigation (by means of steady-state absorption and fluorescence and femtosecond resolved transient absorption techniques) of doxycycline and oxytetracycline (Chart 1) and their complexes with Mg^{2+} cations carried out in aggregates of *p*-dodecyloxybenzyltrimethylammonium bromide (*p*DoTABr) at different pH's are presented in this work.

EXPERIMENTAL SECTION

Chemicals. Doxycycline hyclate (DX) and oxytetracycline dehydrate (OX) (Chart 1) were purchased from Sigma-Aldrich and used without any further purification. All the experiments were carried out under controlled pH conditions of 5.0 and 8.7, obtained by resorting to Britton buffers. The buffers were prepared by mixing an acidic solution (0.04 M H_3BO_3, 0.04 M H_3PO_4, and 0.04 M CH_3COOH) with a 0.2 M solution of NaOH in given ratios. The ionic strength of the final solutions was kept at 5 mM by adding a specific amount of deionized water. $MgCl_2$ anhydrous salt, furnished by Fluka Solutions, was dissolved in pH 5.0 and pH 8.7 buffers for preparation of metal cation Mg^{2+} solutions at needed concentrations.

The cationic surfactant *p*DoTABr (Chart 2) was synthesized and purified in our laboratories.[27,28] The critical micellar concentration (cmc) of the surfactant in buffered water solution was determined at room temperature by surface tension measurements, by using a Fisher 20, du Noüy type, tensiometer to be 9.5×10^{-5} and 1.7×10^{-4} M at pH 5.0 and 8.7, respectively. In particular, *p*DoTABr was dissolved in the buffers at a concentration of 0.03 M to provide micellar solutions where the antibiotics were later dissolved. The drugs were used at concentrations close to 1×10^{-5} M, while different concentrations of Mg^{2+} were added depending on the pH to promote the association process and, thus, to form the metal−drug chelates, whose photophysical properties were to be studied.

Chart 2. Molecular Structure of the *p*-Dodecyloxybenzyltrimethylammonium Bromide (*p*DoTABr) Surfactant

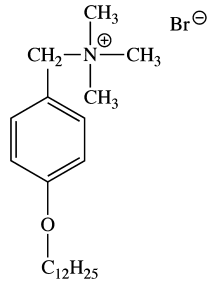

Photophysical Measurements. Absorption spectra were recorded with a PerkinElmer Lambda 800 spectrophotometer, whereas fluorescence emission spectra were recorded with a Fluorolog-2 (Spex, F112AI) spectrophotofluorometer, which accounts both for monochromator response and detector sensitivity. Fluorescence quantum yields (experimental error of ca. 7%) were determined from the emission spectra of the samples, excited at their absorption maximum and keeping the absorbance lower than 0.1 to avoid self-absorption artifices. 9,10-Diphenylanthracene in cyclohexane was used as a standard[29] to calculate the fluorescence quantum yields. Fluorescence quantum yields of the complexes with Mg^{2+} in micellar environment were determined from the fluorimetric titrations of the drugs interacting with *p*DoTABr.

In order to investigate the possible acid−base equilibria of DX in the excited state, an acid−base fluorimetric titration experiment was carried out. A DX stock solution ($\approx 10^{-6}$ M) was prepared in an aqueous solution containing 0.1 M KNO_3. KNO_3 keeps the ionic strength constant. The solution pH was initially adjusted to a value of about 12 by addition of 0.2 N

dx.doi.org/10.1021/jp502278z | J. Phys. Chem. B 2014, 118, 8601−8613

NaOH and then lowered with concentrated HNO_3. The fluorescence emission spectrum (λ_{exc} = 360 nm) of each solution was recorded after adding a negligible acid volume and allowing the solution to equilibrate for 5 min.

The experimental setup for ultrafast transient absorption measurements has been widely described elsewhere.[30,31] Briefly, the 400 nm excitation pulses of ca. 40 fs were generated by an amplified Ti:sapphire laser system (Spectra Physics, Mountain View, CA). The transient absorption setup (Helios, Ultrafast Systems, Sarasota, FL) is characterized by temporal resolution of ca. 150 fs and spectral resolution of 1.5 nm. Probe pulses for optical measurements were produced in the 475−750 nm range by passing a small portion of 800 nm light through an optical delay line (with a time window of 3200 ps) and focusing it into a 2 mm thick sapphire window to generate a white-light continuum. The chirp inside the sample cell was determined by measuring the laser-induced Kerr signal of the *p*DoTABr micellar solution. The femtosecond time-resolved fluorescence spectroscopy employs the up-conversion technique (Halcyone, Ultrafast Systems).[32] The femtosecond laser pulses (the 800 nm and its second harmonic 400 nm) are generated by the same amplified mode-locked Ti−sapphire laser system used in the transient absorption experiments. The second harmonic, after passing through a half wave plate, excites the sample. The remaining fundamental laser beam plays the role of the "optical gate" after passing through an optical delay line with a time window of 3200 ps. The fluorescence of the sample is collected and focused onto a BBO crystal (1.5 mm thickness) together with the delayed fundamental laser beam. The up-converted fluorescence beam is focused into the entrance of a monochromator by a lens, and it is then detected by a photomultiplier connected to a photon counter having an exposure time equal to 2 s at each delay point. The temporal resolution of the time-resolved fluorescence equipment is about 250 fs, whereas the spectral resolution is 5 nm. Absorption and emission measurements were carried out under magic angle conditions, in a 2 mm cell and at an absorbance of 0.3−1.0 at 400 nm. To avoid photoproduct interferences, solutions were stirred during the experiments.

Data Analysis. Acid−base fluorimetric titration data as well as spectrophotometric and fluorimetric Mg^{2+} titration data at pH 8.7 were analyzed by means of the ReactLab Equilibria software (Jplus Comsulting).[33] The program was used to carry out the global fitting of the multivariate data in order to establish the equilibrium constants, concentration profiles, and spectra of the intermediate species. The parameters sum-of-squares (ssq) and deviation standard for the residuals (σr) were used to evaluate the accuracy of the fits.

The association constant (K_{VC}) of the zwitterionic DX (at pH 5.0) to the *p*DoTABr micelles has been determined spectrophotometrically. Mixtures containing variable concentrations of surfactant and constant amounts of the drug ([S] = 2.4×10^{-5} M) have been prepared and their absorption spectra recorded. The association constant K_{VC} has been obtained from eq 1:[34,35]

$$\frac{1}{A - A_0} = \frac{1}{(A_\infty - A_0)\cdot K_{VC}\cdot(c_{p\text{DoTABr}}\text{-cmc})} + \frac{1}{A_\infty - A_0} \quad (1)$$

where A is the measured absorbance at any surfactant concentration, A_0 is the initial absorbance (no added surfactant), A_∞ is the absorbance value at high *p*DoTABr concentration, and ($c_{p\text{DoTABr}}$-cmc) is the concentration of micellized surfactant.

The changes in the fluorescence intensity detected at pH 5.0 at the maximum wavelength depending on the polarity of the drug microenvironment have also been used to evaluate the molar fraction (α) of the zwitterionic DX/OX solubilized into the micelles. α values were determined considering the fluorescence of the solute associated with the micelle (I_{inf}), the fluorescence of aqueous solution of the pure drug (I_0), and the fluorescence intensity of the sample containing the drug and the surfactant (I). The linear graph of $1/\alpha$ as a function of ($c_{p\text{DoTABr}}$-cmc)$^{-1}$ according to eq 2[36] cuts off an intercept on the ordinate axis equal to 1 − (1/P) and shows a slope depending also on q (the micelle aggregation number), υ_0 (the average volume of one micelle), M (the molecular weight of *p*DoTABr), and N_A (the Avogadro number).

$$\frac{1}{\alpha} = \frac{I_{inf} - I_0}{I - I_0} = \frac{qM}{10P(c_{p\text{DoTABr}} - \text{cmc})N_A\upsilon_0} + 1 - \frac{1}{P} \quad (2)$$

P is the partition coefficient of the solute between the W and the Mic phase defined as the ratio of the molar concentration of the solute in the two environments ($P = c_{Mic}/c_W$).

Transient absorption and fluorescence up-conversion data were analyzed using the Surface Xplorer PRO (Ultrafast Systems) software which allowed singular value deconvolution of the 3D surface into principal components (spectra and kinetics) to be performed followed by global analysis (giving lifetimes with an error of ∼10% and decay associated spectra (DAS) of the detected transients).[37] Target analysis assuming successive steps and resulting in the species associated spectra (SAS)[37] was also used to globally fit the acquired absorption data by using Glotaran.[38] Kinetic traces at chosen wavelengths were also analyzed by means of the maximum entropy method (MEM) by means of the MEM EXP Software available online.[39,40] In the maximum entropy method, the experimental decay $A(t)$ was fitted by the following function:

$$A(t) = D_0 \int_{-\infty}^{+\infty} \mathrm{d}\log\tau[g(\log\tau) - h(\log\tau)] \int_{-t_0}^{\min(t,t_f)} \mathrm{d}t' R(t') \mathrm{e}^{-(t_i - t')/\tau} + \sum_{k=0}^{3} (b_k - c_k) \quad (3)$$

where $g(\log\tau)$ and $h(\log\tau)$ are the lifetime distributions that correspond to decay and rise kinetics, respectively, D_0 is a normalization constant, and the polynomial term accounts for the baseline. The instrument response function $R(t)$ is peaked at zero time and is appreciable only on the interval $[-t_0, t_f]$. The fit procedure entailed the maximization of the function Q defined in eq 4:

$$Q = S - \lambda C - \alpha I \quad (4)$$

In eq 4, S is entropy defined as $S(\vec{f}, \vec{F}) = \sum_{j=1}^{M}[f_j - F_j - f_j \ln(f_j/F_j)]$, where f is the image that includes both the g and h lifetime distributions, whereas F is the MEM prior distribution used to incorporate prior knowledge into the solution. C is a measure of the quality of the fit F to the data and corresponds to the χ^2. I is a normalization factor; λ and α are Lagrange multipliers.

dx.doi.org/10.1021/jp502278z | J. Phys. Chem. B 2014, 118, 8601−8613

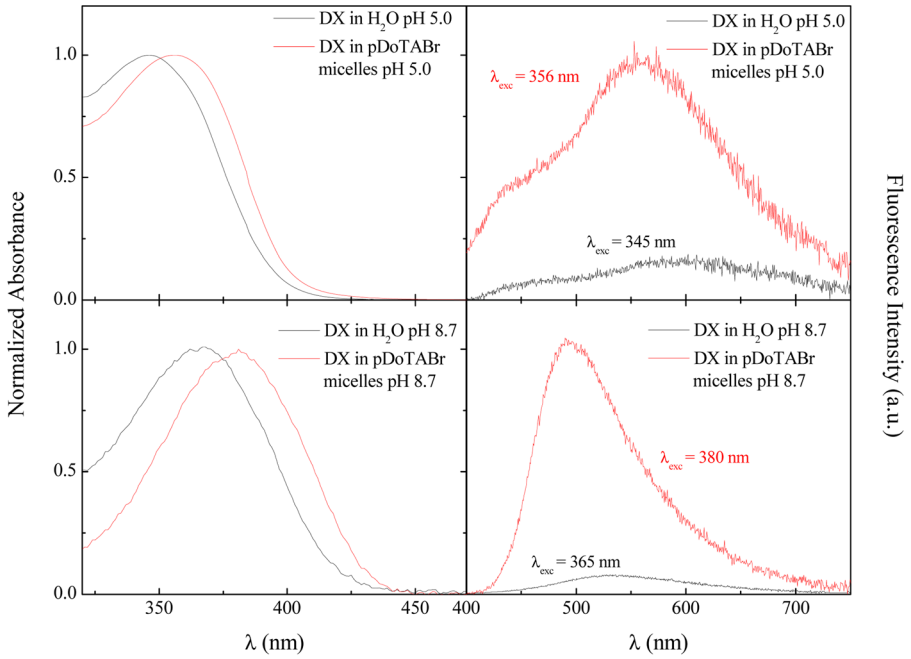

Figure 1. Normalized absorption (left) and emission (right) spectra of ~1×10^{-5} M DX in aqueous solution at pH 5.0 (upper panels) and at pH 8.7 (lower panels) alone (black lines) and in the presence of 3×10^{-2} M *p*DoTABr (red lines).

RESULTS AND DISCUSSION

Absorption and Fluorescence Properties. The absorption and fluorescence properties of DX and OX were investigated in *p*DoTABr micellar medium at pH 5.0 and 8.7. In fact, the pK_a values for DX and OX in the ground state are known to be pK_{a1} = 3.40, pK_{a2} = 7.70, and pK_{a3} = 9.30[41] for DX and pK_{a1} = 3.27, pK_{a2} = 7.32, and pK_{a3} = 9.11[42] for OX. In order to get a deeper insight into the prototropic equilibria occurring in water for these complex systems, a fluorimetric acid–base titration of DX was performed. This experiment revealed the presence of three inflection points and hence three distinct pK_a values at 3.49, 7.88, and 9.60, respectively (see the Supporting Information, Figure S1), which are very close to the pK_a reported in the literature for the ground state of DX. These results suggest that no acid–base re-equilibration takes place in the excited state, as previously found also for the parent molecule tetracycline.[8] From the global analysis of these data, the concentration profiles of the different acid–base forms as a function of pH were obtained (see the Supporting Information, Figure S2) as well as their spectral properties (see the Supporting Information, Figure S3). Bearing this in mind, pH values of 5.0 and 8.7 were the best choice to investigate the neutral-zwitterionic and monoanionic forms of the drugs, respectively, even though it is important to emphasize that it is not possible to have exclusively 100% of one of the different protonated forms, with the pK_a values being too close to each other. The zwitterionic and monoanionic forms are indeed the most interesting deprotonated species of the DX and OX antibiotics, being the ones that most likely can be retrieved in equilibrium in solution under physiological conditions.

The excitation and emission wavelength effect on emission and excitation spectra, respectively, has been evaluated for DX at pH 5.0 and pH 8.7 (see the Supporting Information, Figures S4 and S5). At pH 5.0, where DX is mainly present as zwitterionic species, the emission spectrum shows two emission bands. The excitation spectra, recorded by fixing the wavelength of emission at the two maxima, are overlapped, but the excitation profile shows some differences compared to the absorption spectrum. Moreover, as the excitation wavelength moves to lower energies, the maximum of the long-wavelength band in the fluorescence spectrum shifts toward the blue and the emission of the band at higher energies becomes weaker. This behavior can be explained considering the presence of a small amount of monoanionic DX molecules, in equilibrium with the zwitterionic form. Since the monoanion is much more fluorescent, its contribution adds up to that of the prevailing zwitterion. On the other hand, at pH 8.7, the spectral broadening detected in both the excitation and emission spectra moving to shorter wavelength can still be clarified taking into account the prototropic equilibrium in the ground state and the presence of some zwitterionic molecules.

The peculiar double emission of the zwitterionic DX (Figure 1B) has been questioned in greater detail by means of femtosecond resolved up-conversion measurements, carried out in aqueous solution at pH 5.0. The time-resolved fluorescence spectra (Figure S6, panel B, Supporting Information) show indeed the presence of two bands, rising within 0.5 ps and characterized by different decay kinetics. The band at higher energies experiences a bathochromic shift with time, while decaying very quickly, whereas the band centered at about 600 nm shows a slower decay. The red shift of the hypsochromic band is supposedly due to the fast occurrence of solvation (known to take place in a sub-picosecond time scale in water), as proven by the hydration correlation function found to decay with a time constant of 0.92 ps (Figure S7, Supporting Information). Kinetics traces collected at different wavelengths (Figure S8, Supporting Information) were well fitted by three-exponential functions, whose first component describes the rise of the signal having a time constant of 270 fs, whereas the other two describe the decay of the two bands with lifetimes of 1.1 and 13 ps, respectively. These findings are confirmed by the spectral shapes of the three components (pre-exponential factors at the different wavelengths) obtained by the global fit of the time-resolved fluorescence data (Figure S6, panel C,

dx.doi.org/10.1021/jp502278z | J. Phys. Chem. B 2014, 118, 8601–8613

Table 1. Absorption and Fluorescence Properties of DX and OX and Their Complexes with Mg^{2+} Cations in Aqueous Solutions and in *p*DoTABr Micellar Medium ([*p*DoTABr] = 3×10^{-2} M) at Different pH's[a]

		λ_{abs} (nm)		λ_{em} (nm)		Stokes shift (cm^{-1})		Φ_F	
pH	system	solution	micelles	solution	micelles	solution	micelles	solution	micelles
5.0	DX	345	356	600	555	12 300	10 700	0.000 49	0.0028
	DX–Mg^{2+}	370	367	545[b]	545[b]	8700	8900	0.0058[b]	0.008[b]
	OX	355	360	585	545	11 500	9400	0.000 89	0.0032
	OX–Mg^{2+}	370	370	530[b]	530[b]	7800	7800	0.018[b]	0.028[b]
8.7	DX	365	380	540	495	8900	6100	0.0011	0.011
	DX–Mg^{2+}	370	375	535[b]	510[b]	8300	7100	0.011[b]	0.025[b]
	OX	365	377	530	495	8200	6300	0.0021	0.011
	OX–Mg^{2+}	370	372	530[b]	530[b]	7800	8000	0.016[b]	0.024[b]

[a]Data in solution retrieved from ref 18. Values in micellar medium refer to this work. [b]Emission maximum and fluorescence yield obtained after the last addition of Mg^{2+} in the cuvette.

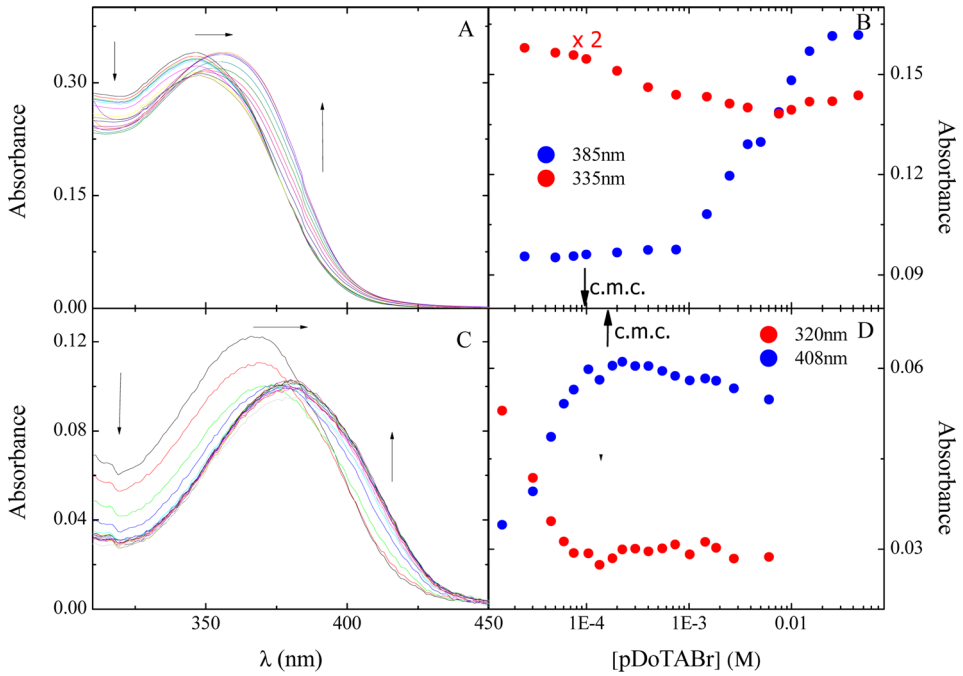

Figure 2. Absorption spectra of DX in aqueous solution at pH 5.0 (A) and at pH 8.7 (C) alone (2.5×10^{-5} and 7.8×10^{-6} M at pH 5.0 and 8.7, respectively) and in the presence of an increasing amount of *p*DoTABr up to 0.045 M at pH 5 and 0.006 M at pH 9. Dependence of the absorbance of DX upon *p*DoTABr concentration at pH 5.0 (B) and at pH 8.7 (D).

Supporting Information). Since the two bands grow in intensity simultaneously by the first hundreds of femtoseconds and then they decay independently, we infer the involvement of two species, which do not show any precursor–successor dynamics. Presumably, some ultrafast keto–enolic tautomerism may be responsible for the two distinct spectral and dynamical contributions taking place within the detected 270 fs rising time (which is close to the temporal resolution of our equipment) or the equilibrium might already exist in the ground state. The fast decay of the species emitting at higher energies is certainly occurring together with and limited by solvent reorganization, taking place in about 1 ps.

It was previously demonstrated in the case of tetracycline[19] that *p*DoTABr does not influence the acid–base equilibria of the drug. The pH values of 5.0 and 8.7, thereof chosen for the present work, should allow one to deal basically with the same protonated form looking both at the absorption and emission properties of the DX and OX drugs in water as well as in the organized medium.

Figure 1 shows the normalized absorption and emission spectra recorded for DX in the presence of *p*DoTABr micelles in comparison with those measured in buffered water, whereas the results obtained for OX are shown in the Supporting Information, Figure S9; all the collected data are summarized in Table 1. The absorption spectra are bathochromically shifted by the presence of the micelles, while the emission is significantly blue-shifted and an increase in the fluorescence quantum yield is observed both at pH 5.0 and at 8.7. A strong reduction of the Stokes shift is therefore observed on going from the bare solution to the organized medium. A very similar effect induced by *p*DoTABr micelles[19] was observed on the spectra of the parent molecule tetracycline. However, from a quantitative point of view, the fluorescence enhancement observed for DX and OX in the micellar environment is much more significant than that observed for tetracycline. The fluorescence quantum yields (Φ_F in Table 1), which increased just by a factor of 1.3–1.4 for tetracycline at pH 5.0 and 8.7 in the presence of *p*DoTABr,[19] are here found to be higher by a factor of 6–10 in

dx.doi.org/10.1021/jp502278z | J. Phys. Chem. B 2014, 118, 8601–8613

the case of DX and OX in the confined medium with respect to the corresponding values in buffered solution. The enhancement is comparatively more important for DX than for OX.

The reasons underlying this unexpected behavior (considering the very similar molecular structures of tetracycline, DX, and OX) could be thoroughly understood by means of spectrophotometric and fluorimetric titrations, looking carefully at the spectral modifications induced by the increasing amounts of *p*DoTABr to DX and OX aqueous solutions. Figure 2A shows the absorption spectra of DX alone and in the presence of different concentrations of *p*DoTABr at pH 5.0. Interestingly, in the presence of low surfactant concentrations, the absorption band centered at 345 nm is bathochromically and hypochromically shifted, while when a higher *p*DoTABr amount is reached a different trend is observed, with the red shift being coupled with a hyperchromic effect.

An analogous double trend in the spectral modifications can be observed looking at the fluorimetric titration carried out at pH 5.0 and shown in Figure 3A. On going from the black

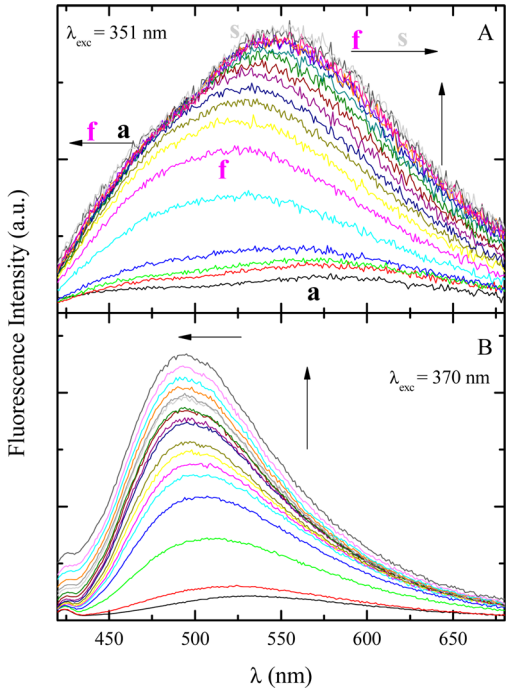

Figure 3. Fluorescence spectra of DX (7.8×10^{-6} M) in aqueous solution at pH 5.0 (A) and at pH 8.7 (B) alone and in the presence of an increasing amount of *p*DoTABr up to 0.012 M at pH 5.0 and 0.006 M at pH 8.7.

emission spectrum (a) to the magenta one (f, corresponding to a 3.8×10^{-4} M concentration of *p*DoTABr added), a hypsochromic shift occurs. Thereafter, from spectrum f to the gray spectrum s, an inverse trend (spectral red shift) is observed. In fact, for the micellar media obtained in water buffered at pH 5.0, a cmc of 9.5×10^{-5} M has been measured. Therefore, the initially observed emission blue shift may be related to a one-to-one interaction of DX with the surfactant, while the subsequent red shift may be due to the inclusion of the zwitterionic DX in the formed *p*DoTABr micelles. This hypothesis is in agreement with the evidence that the major variations in the DX absorption at pH 5.0 are observed at surfactant concentrations higher than the cmc value (Figure 2B). Moreover, in the case of tetracycline, where just an interaction with the micellar surface was supposed to occur, only a single trend of spectral variations (absorption red hypochromic shift and fluorescence blue shift) was observed even above the cmc during the spectrophotometric and fluorimetric investigation.[19] In the case of OX, an intermediate behavior is observed: a double trend in the evolution of the fluorimetric data at different *p*DoTABr concentrations is still present (see the Supporting Information, Figure S10, panel A) even though less evident than that found investigating DX.

The association constant, K_{VC}, of the zwitterionic DX to the *p*DoTABr micelles was estimated by monitoring the changes in the absorbance of its UV−vis spectrum at 385 nm and by fitting the data according to eq 1 (see Figure 4). The calculated K_{VC}

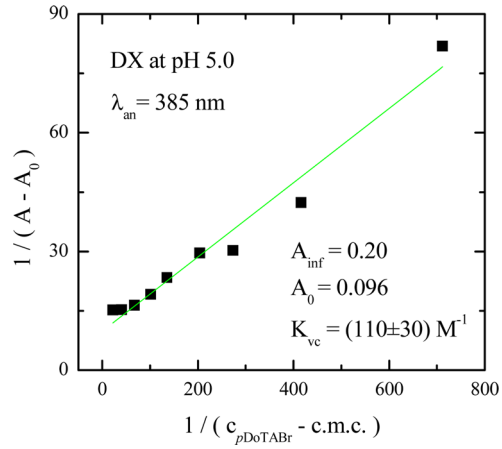

Figure 4. Estimation of the association constant, K_{VC}, of DX at pH 5.0 according to eq 1 by monitoring the changes in the absorption spectrum.

value of 110 ± 30 M^{-1} indicates an efficient inclusion of DX into the micellar aggregates.[34] The less relevant variations in the absorption spectrum of OX in the presence of increasing amounts of the surfactant prevented us from a spectrophotometric estimation of K_{VC} for this molecule; to this end, the more sensitive fluorimetric spectroscopy has been used. Linearization of the dependence of $1/\alpha$ versus the surfactant concentration is shown in the Supporting Information, Figures S11 and S12, in the case of DX and OX, respectively; with α being the molar fraction of the zwitterionic tetracycline solubilized into the micelles calculated from the fluorimetric titration data (see details in the Experimental Section). The determination of the partition coefficient gives values of $P = 76 \pm 3$ for DX and $P = 2.1 \pm 0.6$ for OX. The high P value found for DX is in fair agreement with the efficient association constant (K_{VC}) retrieved from the absorption data, whereas the interaction of the more hydrophilic OX drug with the micelles can be considered rather weak.[36]

Extremely different results, and thus of utmost interest, have been obtained from the spectrophotometric and fluorimetric titrations carried out at pH 8.7. Figure 2C reports the absorption spectra of DX in aqueous solution at pH 8.7 recorded upon successive additions of the surfactant. It is evident that in this case just one trend of spectral modifications is revealed: the bathochromic shift accompanied by a reduction of the DX absorbance. Similarly, only a blue shifting increase in the fluorescence intensity may be noted looking at the fluorimetric titration (Figure 3B). Moreover, the graph in Figure 2D, showing the dependence of the absorbance on the

dx.doi.org/10.1021/jp502278z | J. Phys. Chem. B 2014, 118, 8601−8613

*p*DoTABr concentration, is revealing: all the variations occur before the cmc value (1.7×10^{-4} M) after which no significant evolution takes place. These findings point to a completely different behavior of the charged monoanionic DX (the form present at pH 8.7) with respect to the neutral-zwitterionic one. In fact, while the hydrophobic zwitterion is able to be included in the micellar aggregate, the highly polar monoanion exhibits a strong electrostatic interaction with the cationic surfactant when it is individually present in solution but probably it is not anymore sympathetic to the micellar inner core. This explains why no spectral modifications are revealed at high surfactant concentrations, after the supramolecular micellar structures have been formed. A similar behavior has been found in the case of OX. Interestingly, the global fitting of the spectrophotometric titrations carried out at pH 8.7 revealed a relevant value for the association constants of DX and OX with the *p*DoTABr monomeric surfactant (log K_{ass} = 4.80 ± 0.02 and 4.25 ± 0.02 for DX and OX, respectively). We believe that the different behavior of the zwitterionic and monoanionic forms is really promising: the pH becomes an input to control the possible inclusion of these molecules inside the micelle.

It is well-known that the interaction with positively charged metal ions is crucial in determining the biological functioning of the tetracycline drugs. For this reason, we decided to investigate if the complexation with magnesium, already characterized in aqueous solution in previous works,[15,18] still occurs for the investigated DX and OX in the *p*DoTABr micellar medium which could be used as a pH controlled drug delivery system. Absorption and emission spectra of both DX and OX in the presence of the micelles are significantly affected by the addition of increasing amounts of Mg^{2+}, pointing to an interaction that is efficiently operative. The results obtained from the fluorimetric measurements are shown as an example in the Supporting Information, Figure S10, and in Figure 5 at pH 5.0 and 8.7, respectively. Looking qualitatively at these data, one important consideration can be made by comparing the behavior of the two molecules. In panel A of both figures, where data relative to DX are shown, the first additions of Mg^{2+} have no effect on the fluorescence: only when a relevant amount of the cation is added the fluorescence intensity starts to increase. On the contrary, when Mg^{2+} is added to solutions of OX in micellar medium at both pH's (panel B of both figures), a growth of the fluorescence intensity is immediately observed even after the very first additions. This different behavior of the two drugs may be due to their different inclusion inside the micellar core (at pH 5.0) and slightly different interaction with the surfactant (at pH 8.7). In fact, DX has been found to show a greater affinity to surfactants and micelles with respect to OX and therefore its interaction with magnesium ions may be somehow more hindered by the presence of *p*DoTABr. However, the association constants for the interaction with the metal ions calculated by the titrations at pH 8.7 (reported in Table 2) even though reduced by the presence of the surfactant with respect to those in solution[18] are still extremely high. Moreover, an attentive analysis of the spectral shapes obtained for the complexes by the global fitting of the spectrophotometric titrations revealed that for both DX and OX the first Mg^{2+} complexation involves the A ring and only the second the BCD system. In the case of DX, this specific complexation mechanism, different from the one operative in solution,[18] is probably determined by the existing interaction between the cationic surfactant and the BCD lower peripheral region which happens to be negatively charged at pH 8.7: being involved in the interaction with the positively charged surfactant heads, this particular site thus becomes less accessible to the Mg^{2+} ions.

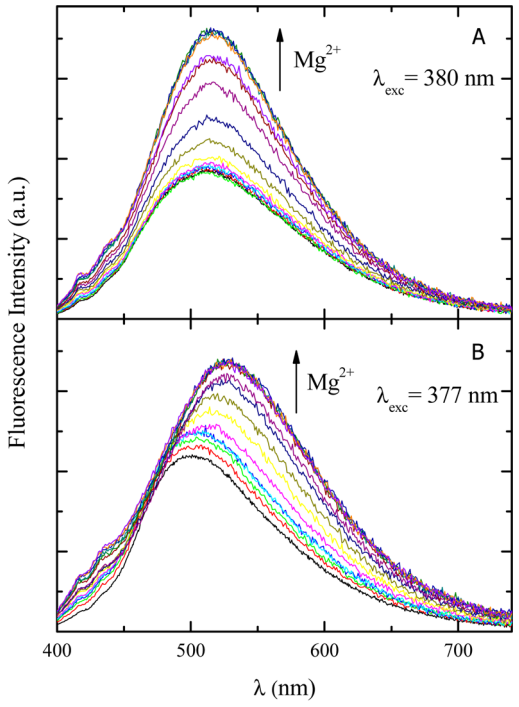

Figure 5. Fluorescence spectra of 8.0×10^{-6} M DX (A) and 1.0×10^{-5} M OX (B) in a micellar environment at pH 8.7 ([*p*DoTABr] = 3×10^{-2} M) alone and in the presence of an increasing amount of Mg^{2+} up to a concentration of 0.06 M.

Table 2. Association Constants (K_{ass}) Obtained by Absorption Titrations and Interaction Sites of the Complexes between DX/OX and Mg^{2+} Cations in Aqueous Solution and in *p*DoTABr Micellar Medium ([*p*DoTABr] = 3×10^{-2} M) at pH 8.7

			log K_{ass}		
pH	system	complex	solution[a]	micelle	site
8.7	DX–Mg^{2+}	1:1	4.19 ± 0.01	2.53 ± 0.05	A
		1:2	1.85 ± 0.04	1.12 ± 0.05	BCD
	OX–Mg^{2+}	1:1	4.01 ± 0.01	3.24 ± 0.05	A
		1:2	1.87 ± 0.05	1.36 ± 0.07	BCD

[a]Data in solution retrieved from ref 18. Values in micellar medium refer to this work.

Femtosecond Transient Absorption. In order to get an insight into the effect of the micellar medium on the excited state dynamics of DX and OX, femtosecond resolved transient absorption spectroscopy has been employed considering the low fluorescence quantum yields of the investigated systems and the fast deactivation of tetracyclines[8] and their complexes with Mg^{2+}.[18]

The time-resolved absorption spectra obtained for zwitterionic DX studied at pH 5.0 in solution, in micellar medium and also in the presence of Mg^{2+} cations, are shown in panel B of Figures 6, 7, and 8, respectively. The spectra recorded in solution (Figure 6B) show positive signals of transient absorption in the spectral range below 570 nm and a negative broad band of stimulated emission centered around 690 nm. The maximum of this stimulated emission band is red-shifted in

dx.doi.org/10.1021/jp502278z | J. Phys. Chem. B 2014, 118, 8601–8613

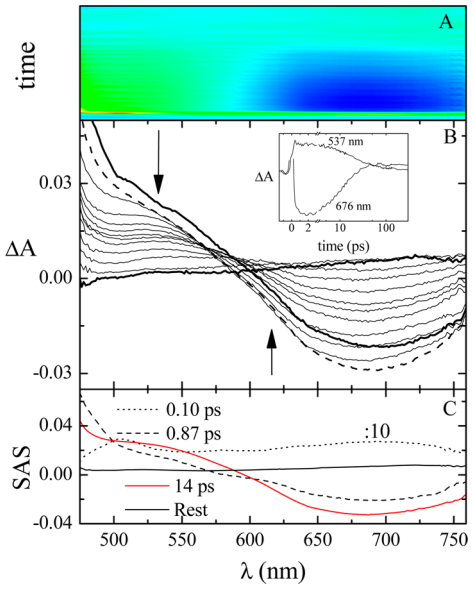

Figure 6. Pump−probe absorption spectroscopy of DX in aqueous solution at pH 5.0 (λ_{exc} = 400 nm): (A) contour plot of the experimental data; (B) time-resolved absorption spectra at increasing delays after the laser pulse (the spectra relative to the shortest and longest delay times are represented by thicker lines); insets: decay kinetics recorded at meaningful wavelengths; (C) species associated spectra (SAS) of the decay components obtained by target analysis.

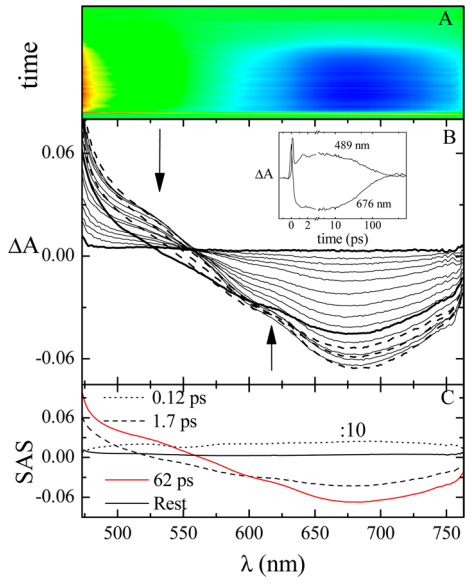

Figure 7. Pump−probe absorption spectroscopy of DX in a micellar environment at pH 5.0 (λ_{exc} = 400 nm; [*p*DoTABr] = 3 × 10^{-2} M): (A) contour plot of the experimental data; (B) time-resolved absorption spectra at increasing delays after the laser pulse (the spectra relative to the shortest and longest delay times are represented by thicker lines); insets: decay kinetics recorded at meaningful wavelengths; (C) species associated spectra (SAS) of the decay components obtained by target analysis.

comparison to the steady-state fluorescence because of the more intense excited state absorption below 600 nm. The spectra are not significantly affected by the presence of the micelles (Figure 7B), while the interaction with Mg^{2+} ions in the organized medium (Figure 8B) induces an evident blue shift of the stimulated emission band which is centered around

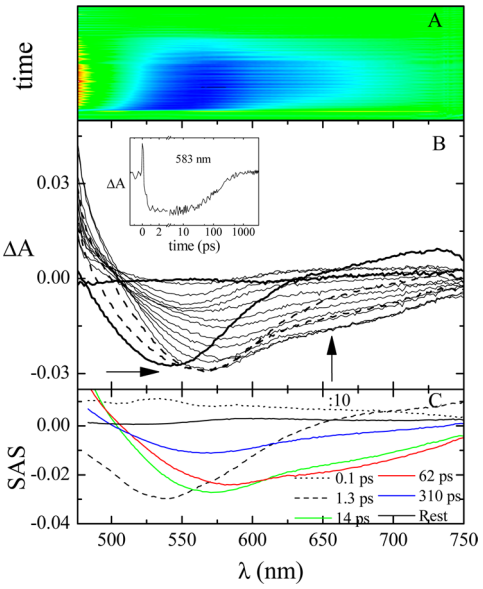

Figure 8. Pump−probe absorption spectroscopy of DX in a micellar environment at pH 5.0 (λ_{exc} = 400 nm; [*p*DoTABr] = 3 × 10^{-2} M) in the presence of Mg^{2+}: (A) contour plot of the experimental data; (B) time-resolved absorption spectra at increasing delays after the laser pulse (the spectra relative to the shortest and longest delay times are represented by thicker lines); insets: decay kinetics recorded at a meaningful wavelength; (C) species associated spectra (SAS) of the decay components obtained by target analysis.

570 nm but still exhibits an evident shoulder around 680 nm. This behavior recalls the important hypsochromic shift observed during the fluorimetric titration with magnesium of the zwitterionic DX in aqueous solution.[18] The insets of panel B in the Figures 6, 7, and 8 show the decay and growing kinetics recorded at meaningful wavelengths in the spectral regions of positive and negative absorbance, respectively.

The analysis of the kinetic traces has been carried out through two different methods of data mining: the global and target analysis furnishing a discrete number of transients, their associated lifetimes, and spectral shapes and the maximum entropy method (MEM) admitting the contribution of an unlimited number of transients. The synergistic use of these refined data treatments has been an added value in order to extract all the possible information from the obtained results and to be confident about its reliability. All the results obtained by using the target analysis are shown in panel C of the figures, and they are summarized in Table 3; those achieved by using the maximum entropy method are shown in Figure 9. MEM was successfully applied to the analysis of nanosecond resolved fluorescence kinetics of fluorophores in microcrystalline solid phases,[43,44] in microheterogeneous media such as polymeric matrixes,[45,46] micelles,[47−49] and proteins.[50,51] To the best of our knowledge, application of the MEM analysis to femtosecond pump−probe spectroscopy is quite rare because ultrafast kinetic data often contain oscillatory signals superimposed on the exponential background decay signals.[52] This work, presenting the results of the MEM analysis performed on the most free from noise kinetic signals, reveals how a micelle environment affects the ultrafast relaxation dynamics of DX species.

The global and target analysis of the ultrafast spectroscopic data for DX in aqueous solution at pH 5.0 revealed the presence of four components: the first three characterized by

dx.doi.org/10.1021/jp502278z | J. Phys. Chem. B 2014, 118, 8601−8613

Table 3. Spectral and Kinetic Properties of the Excited States of DX, OX, and Their Complexes (1:1 and 1:2) with Mg^{2+} in Aqueous Solution and in *p*DoTABr Micellar Medium at Different pH's (λ_{exc} = 400 nm; [*p*DoTABr] = 3×10^{-2} M)[a] Obtained by Target Analysis

pH	system	solution		micelle		assignment
		λ (nm)	τ(ps)	λ (nm)	τ(ps)	
5.0	DX	505(+),695(+)	0.10	520(+), 690(+)	0.12	$Solv._i$
		695(−)	0.87	675(−)	1.7	$Solv._d$
		685(−)	14	680(−)	62	S_1(DX)
		720(+)	Rest	710(+)	Rest	T_1(DX)
	$DX-Mg^{2+}$			530(+)	<0.1	$Solv._i$
		550(−)	1.3	540(−)	1.3	$Solv._d$
		585(−)	18	575(−)	14	S_1(DX-Mg^{2+};1:1A) H_2O
				585(−), 650(−)	62	S_1(DX) micelle
		580(−)	170	570(−)	310	S_1(DX-Mg^{2+};1:2A,BCD) H_2O
				595(+)	Rest	T_1(DX)
	OX	500(+)	0.12	500(+)	0.15	$Solv._i$
		590(−)	2.2	575(−)	2.9	$Solv._d$+VC
		680(−)	18	675(−)	48	S_1(OX)
		Broad	Rest	Broad	Rest	T_1(OX)
	$OX-Mg^{2+}$	530(−)	0.56	535(−)	1.3	Solv.
		550(−)	32	555(−)	27	S_1(OX-Mg^{2+};1:1A) H_2O
		560(−)	300	565(−)	330	S_1(OX-Mg^{2+};1:2A,BCD) H_2O
				605(+)	Rest	T_1
8.7	DX	505(−), 735(+)	0.17	495(−), 670(+)	0.14	$Solv._i$
		550(−), 740(+)	3.4	520(−), 740(+)	2.8	$Solv._d$+VC
		575(−)	32	525(−), 740(+)	30	S_1(DX1)
		550(−), 730(+)	220	535(−), 740(+)	170	S_1(DX2)
		730(+)	Rest	broad	Rest	T_1
	$DX-Mg^{2+}$	545(−)	0.69	515(−), 720(+)	0.12	$Solv._i$
				545(−), 715(+)	2.6	$Solv._d$+VC
				550(−), 710(+)	24	S_1(DX-Mg^{2+};1:1A) H_2O
		570(−)	200	550(−), 715(+)	400	S_1(DX-Mg^{2+};1:2A,BCD) H_2O
				broad	Rest	T_1
	OX	485(−), 725(+)	0.16	485(−), 660(+)	0.15	$Solv._i$
		560(−), 730(+)	2.7	520(−), 740(+)	3.7	$Solv._d$+VC
		595(−)	24	530(−), 740(+)	33	S_1(OX1)
		565(−)	230	540(−), 740(+)	250	S_1(OX2)
		710(+)	Rest	580(+)	Rest	T_1
	$OX-Mg^{2+}$	535(−)	0.48	515(−), 675(+)	0.10	$Solv._i$
				550(−), 725(+)	8.0	$Solv._d$+VC
		560(−)	20	550(−), 720(+)	58	S_1(OX-Mg^{2+};1:1A) H_2O
		570(−)	270	555(−), 715(+)	480	S_1(OX-Mg^{2+};1:2A,BCD) H_2O
				Broad	Rest	T_1

[a]Data in solution for the complexes retrieved from ref 18.

lifetimes of 0.10 ps (S), 0.87 ps (S′), 14 ps (M), and the fourth one (Rest) lasting longer than the time window of 3200 ps covered by the pump−probe technique. The lifetimes of the first three components are in fair agreement with those revealed by the up-conversion measurements. The first two short living transients (S and S′) are assignable to solvent relaxation dynamics, which in water takes place on a sub-picosecond time scale.[53] Moreover, solvation is known to show a time dependence which is biexponential concerning both the inertial and diffusive parts of the response ($Solv_i$ and $Solv_d$ in Table 3).[54] However, as previously pointed out, a contribution of a tautomeric form of the drug in the S′ decay cannot be excluded. The medium lived component (M) of 14 ps, characterized by a spectrum showing a negative band of stimulated emission centered at 690 nm (Figure 6C), is ascribed to the relaxed S_1 state of DX. In fact, in previous works,[8,17] the lowest excited singlet state of tetracyclines in solution has been found to decay in tens of picoseconds. The Rest component may be due to the low efficient population of a long living triplet state, as observed also in analogous compounds.[8]

In the case of zwitterionic DX in the presence of micelles, the global fitting revealed the presence of the same number of components with similar associated spectra but with lengthened lifetimes. In particular, as expected,[55] the second component ascribed to diffusive solvation is slightly slowed down ($\tau_{S'}$ = 1.7 ps in micellar medium compared to 0.87 ps in solution). However, the most important effect of the micellar medium is on the lifetime of the S_1 state (M component), found to be of 62 ps, 4 times longer than the analogous component in solution. This finding seems to confirm the steady-state evidence of an inclusion of the zwitterionic DX inside the confined and restrained environment of the micelles that leads to a significant slowdown in the excited state deactivation. In this context, the comparison with the results obtained for TC and OX is revealing. In fact, in the case of the zwitterionic TC, the S_1 lifetime in water and in a *p*DoTABr micellar medium was found to be 22 and 24 ps, respectively,[19] with the unaffected dynamics being a clear signature of TC molecules remaining outside the micellar core. For OX investigated at pH 5.0 (see Table 3), once again an intermediated behavior is observed: the S_1 lifetime is increased by a factor of 2.7 (from 18 to 48 ps) on

dx.doi.org/10.1021/jp502278z | J. Phys. Chem. B 2014, 118, 8601−8613

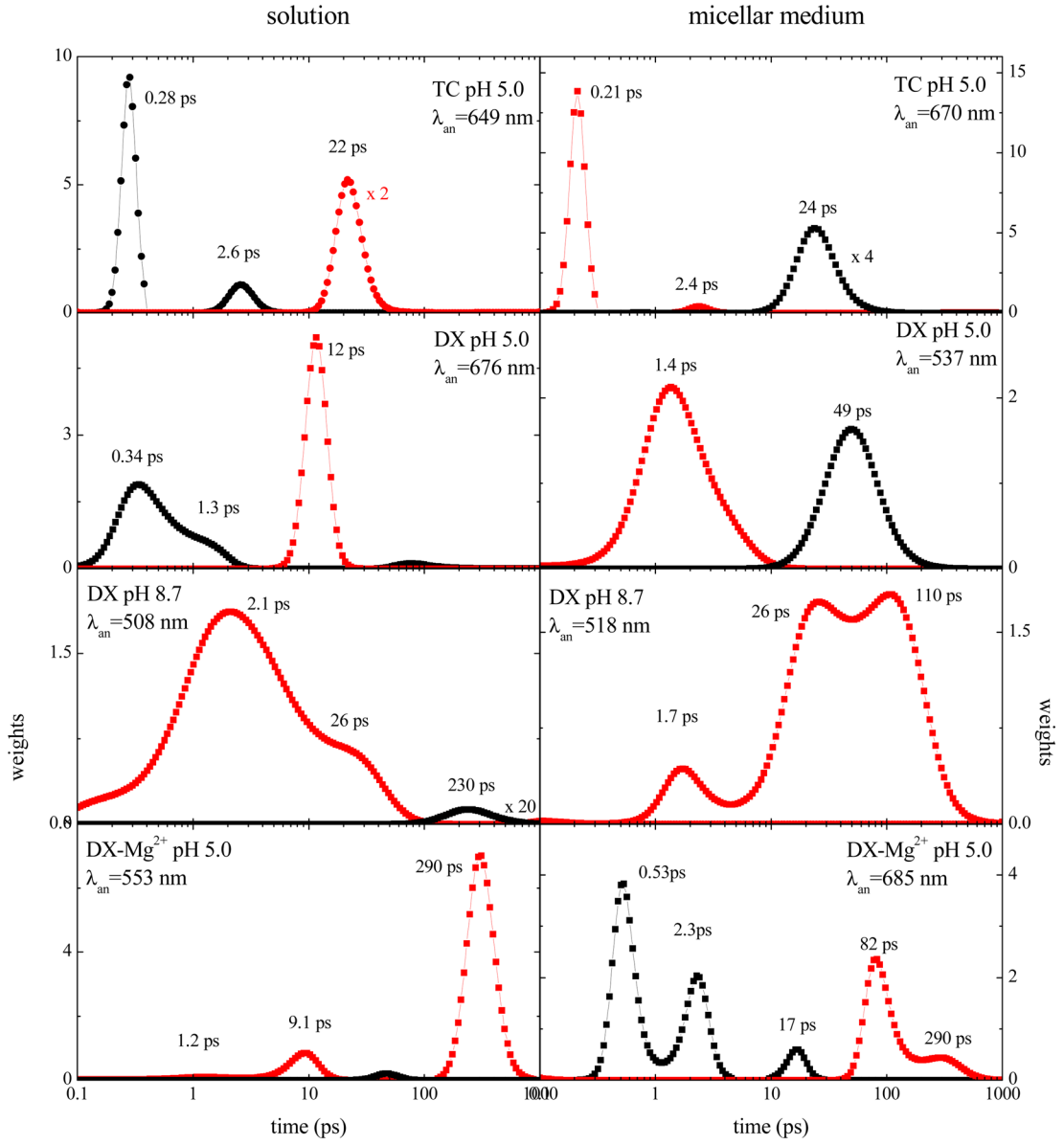

Figure 9. Results of the analysis of the femtosecond transient absorption kinetics at significant wavelengths by the maximum entropy method for TC at pH 5.0, DX at pH 5.0 and pH 8.7, and DX−Mg^{2+} at pH 5.0, both in aqueous solution and in micellar medium. The red and black distributions represent growth and decay contributions, respectively.

going from the pure solution to the organized environment. This result agrees with the less efficient but still occurring inclusion of the zwitterionic OX within the micelles with respect to DX.

Further information on the transient lifetime distribution is obtained by comparing the results of the MEM analysis carried out on the kinetic data of the zwitterionic TC and DX in solution and in micellar medium (see Figure 9). In the case of TC, the MEM analysis reveals that the data in both environments are well fitted by three main sharp sets of lifetime distributions centered at 0.28/0.21, 2.6/2.4, and 22/24 ps, respectively, in excellent agreement with the results of a previous study.[19] Just a small enlargement is observed on going from the solution to the micelles for the peak detected around 20 ps (the fwhm increases from 13 to 22 ps). When data collected for DX are considered, much broader distributions were found through the MEM analysis in the organized medium with respect to the pure solution. In particular, for the peak describing the lifetime distribution of the S_1 state (found to be centered at 12 and 49 ps in the two environments), a fwhm of 6 ps was calculated in water and 65 ps in the presence of the micelles. This broadening reflects the microheterogeneous properties of a micellar medium.

When Mg^{2+} ions are present in a micellar solution of the zwitterionic DX, a higher number of components (five components of <0.1, 1.3, 32, 97, and 310 ps besides the Rest; see Table 3) are necessary to well reproduce the experimental trend of the kinetics through the global fitting. The reliability of the results of this complex fitting was confirmed by MEM analysis (shown in the lower right panel of Figure 9) which also evidenced the presence of five peaks at similar times in the lifetime distribution functions. The <0.1 and 1.3 ps components are assigned to the inertial and diffusive solvation. The assignment of the other three components has been supported by the careful consideration of their spectral shapes and lifetimes compared with those resulting from the

dx.doi.org/10.1021/jp502278z | J. Phys. Chem. B 2014, 118, 8601−8613

measurements of other related systems (DX in micelles and DX−Mg^{2+} in solution, also reported in Table 3). The spectral and kinetic properties of the 14 and 310 ps components resemble those of the 1:1 and 1:2 DX−Mg^{2+} complexes in water solution, while the 62 ps transient shows an evident shoulder around 650 nm in its associated SAS recalling the spectral shape characteristic of DX included in the micelles. The simultaneous detection of these species from the ultrafast investigation indicates that the presence of magnesium is able to extract part of the DX embedded in the core of the micelles and therefore to induce the release of its biologically active form (DX−Mg^{2+}) into the aqueous solution. For OX−Mg^{2+} investigated in a micellar environment at pH 5.0 (see Table 3), the lack of the term relative to OX trapped inside the micelle can be understood considering the reduced affinity of this molecule for the micelle (lower *P*) and increased affinity for Mg^{2+} ions (see Table 2) with respect to DX. In fact, in this case, the global and target analysis revealed that, besides the transient of 1.3 ps (S) related to solvation, two more exponential components of 27 (M) and 330 ps (L) together with Rest are needed to satisfactorily fit the experimental data. These M and L components are assignable to the 1:1 and 1:2 OX−Mg^{2+} complexes in solution.

Femtosecond transient absorption spectra recorded for DX at pH 8.7 show a negative band of stimulated emission centered around 540 nm and a positive band of transient absorption around 730 nm (see the Supporting Information, panel B of Figures S11 and S12). Very interestingly, the global and target analysis indicate that four components (together with the Rest) must be used to obtain a good fitting both in solution and in micellar medium characterized by very similar lifetimes of 0.17/0.14 (S), 3.4/2.8 (S′), 32/30 (M), and 220/170 (L) ps, respectively (see Table 3). The negligible effect of the presence of the micelles on the lifetimes is in perfect agreement with the results of the steady-state investigation, which suggests that no inclusion of the anionic DX within the hydrophobic surfactant tails takes place. The S and S′ components reflect the occurrence of inertial and diffusive solvent relaxation. However, the slightly longer S′ lifetime with respect to that observed during the measurements carried out at pH 5.0 is supposedly due to the concomitant vibrational cooling (VC) taking place for the monoanionic DX (its red-shifted absorption spectrum with respect to the zwitterionic form (see Figure 1) implies that the 400 nm excitation occurs with a larger excess of vibrational energy). Besides the M component of tens of picoseconds (assigned to the S_1 state of DX similarly to what discussed at pH 5.0), an additional longer lived transient of hundreds of picoseconds is detected at basic pH, ascribable to a differently protonated or tautomeric form of the lowest excited singlet state. In fact, the evidence of a keto−enolic tautomerism in tetracyclines involving the hydroxyl and ketonic groups of the lower peripheral region of the BCD rings has been foreseen by semiempirical and quantum mechanical calculations[9,10] and experimentally observed in DX in aqueous solution at different pH's.[11] The spectral shapes obtained from the global analysis for the most important M and L components (see the Supporting Information, panel C of Figures S11 and S12) indicate that their characteristic stimulated emission band appears blue-shifted on going from the solution to the micellar medium, in agreement with the large hypsochromic shift observed during the fluorimetric steady-state titration (Figure 3B) due to the interaction with the surfactant. It has to be noted that the MEM applied to the kinetic data at similar wavelengths of analysis at pH 8.7 both in solution and in micellar medium (Figure 9) has unambiguously shown that the weight of the L component becomes significantly higher in this latter. This finding can be explained considering that the association with the cationic surfactant of the monoanionic DX alters the keto−enolic equilibrium, since DX most likely interacts with the head of *p*DoTABr through the negatively charged (after the second deprotonation at pK_{a2} = 7.70) lower peripheral region, involved also in the tautomerism. Evidence of an analogous excited state behavior has been obtained in the case of the monoanionic OX, and the results are summarized in Table 3. Experimental findings pointing to a modulation induced by the micellar medium of the ground or excited state keto−enolic intramolecular proton transfer in other organic conjugated compounds have been recently reported in the literature.[56,57]

It is worth pointing out that the spectral shapes detected by means of femtosecond transient absorption measurements, compared to the same data in pure aqueous solution, confirm the presence of the same acid−base form as in water at both pH 5.0 and 8.7.

CONCLUSIONS

A spectroscopic investigation of DX and OX has been carried out by using steady-state absorption and fluorescence techniques, and femtosecond transient absorption in aqueous solution and in micellar medium attained by means of a cationic quaternary ammonium surfactant.

The results of the spectrophotometric and fluorimetric titrations suggest that the neutral-zwitterionic form of the two drugs (prevailing at pH 5.0) can be enclosed within the hydrophobic micellar core, while the monoanionic form (prevailing at pH 8.7) just shows a significant one-to-one interaction with the positively charged surfactant. Therefore, it is the pH of the solution to control the inclusion of DX and OX into the micelles. In fact, the pH rules the net charge and therefore hydrophobicity and affinity for the micelle inner portion of the guest DX and OX molecules. The partition coefficients calculated for the two molecules at pH 5.0 indicate that DX is more preferentially distributed in the supramolecular system with respect to OX, and surprisingly that both compounds behave differently from the parent tetracycline despite their similar molecular structures.

Femtosecond transient absorption measurements have revealed that the lifetime of the lowest excited singlet state is strongly lengthened only when the molecules are placed inside the micelle. The maximum entropy method has been successfully applied to these data and indicates that the lifetime distribution is significantly broadened for the zwitterionic species, reflecting the microheterogeneous nature of the micellar medium. Differently, the interaction of the DX and OX monoanionic forms with the surfactant influences the position of the keto−enolic equilibrium, modifying the relative amount of the two tautomers retrieved by the analysis of the ultrafast spectroscopic data obtained at pH 8.7.

The drugs, even when included within the micelles, are still able to strongly interact with Mg^{2+} cations, as has been proven by the spectral modifications observed after magnesium salt addition to micellar solutions of the different tetracyclines. Moreover, the spectral and kinetic properties of the transients detected during the femtosecond resolved investigation carried out in the presence of magnesium suggest that DX and OX are

dx.doi.org/10.1021/jp502278z | J. Phys. Chem. B 2014, 118, 8601−8613

efficiently pulled out of the micelles as Mg^{2+} complexes which may be retrieved in aqueous solution.

In conclusion, the present spectroscopic study puts forward the potential promising use of ammonium surfactant micelles embedding DX/OX molecules as smart host−guest supramolecular systems allowing a pH controlled inclusion of DX and OX and a Mg^{2+} induced release of them. Finally, the sensitivity of the absorption and emission spectra of tetracycline, doxycicline, and oxytetracycline toward pH, metal cations, and surfactants makes them promising probes for the development of chemical artificial intelligence.[38]

■ ASSOCIATED CONTENT

Supporting Information

Detailed results of fluorimetric acid−base titration, concentration profiles, absorption and emission spectra of differently protonated substrates, femtosecond up-conversion fluorescence measurements (spectra and decay kinetics), fluorescence titrations by Mg^{2+}, determination of partition coefficients (by eq 2), and femtosecond excited state absorption data. This material is available free of charge via the Internet at http://pubs.acs.org.

■ AUTHOR INFORMATION

Corresponding Author

*E-mail: fausto.elisei@unipg.it. Phone: +39 075 585 5588. Fax: +39 075 585 5598.

Author Contributions

The manuscript was written through contributions of all authors. All authors have given approval to the final version of the manuscript. All authors contributed equally.

Notes

The authors declare no competing financial interest.

■ ACKNOWLEDGMENTS

The authors are grateful to Simona Fontanella for her contribution to the surface tension measurements during her thesis work. The authors thank the Ministero per l'Università e la Ricerca Scientifica e Tecnologica, MIUR (Rome, Italy) [PRIN "Programmi di Ricerca di Interesse Nazionale" 2010−2011, n. 2010FM738P] and Regione Umbria (POR FSE 2007−2013, Risorse CIPE, Perugia, Italy) for fundings. The authors are grateful to Prof. Anna Spalletti for stimulating discussions.

■ REFERENCES

(1) Nelson, M. L.; Ismail, M. Y. *The Antibiotic and Nonantibiotic Tetracyclines*; Elsevier: Amsterdam, 2007.

(2) Griffin, M. O.; Fricovsky, E.; Ceballos, G.; Villarreal, F. Tetracyclines: a Pleitropic Family of Compounds with Promising Therapeutic Properties. Review of the Literature. *Am. J. Physiol.* **2010**, *299*, C539−C548.

(3) Bahrami, F.; Morris, D. L.; Pourgholami, M. H. Tetracyclines: Drugs with Huge Therapeutic Potential. *Mini-Rev. Med. Chem.* **2012**, *12*, 44−52.

(4) Schmitt, M. O.; Schneider, S.; Nelson, M. L. Novel Insight into the Protonation−Deprotonation Equilibria of Tetracycline and Several Derivatives in Aqueous Solution. II. Analysis of the pH-Dependent Fluorescence Spectra by the SVD Technique. *Z. Phys. Chem.* **2007**, *221*, 235−271.

(5) Rigler, N. E.; Bag, S. P.; Leyden, D. E.; Sudmeier, J. L.; Reilley, C. N. Determination of a Protonation Scheme of Tetracycline Using Nuclear Magnetic Resonance. *Anal. Chem.* **1965**, *37*, 872−875.

(6) Qiang, Z.; Adams, C. Potentiometric Determination of Acid Dissociation Constants (p*Ka*) for Human and Veterinary Antibiotics. *Water Res.* **2004**, *38*, 2874−2890.

(7) Babic, S.; M. Horvat, A. J.; Mutavdzic Pavlovic, D.; Kastelan-Macan, M. Determination of p*Ka* Values of Active Pharmaceutical Ingredients. *Trends Anal. Chem.* **2007**, *26*, 1043−1061.

(8) Carlotti, B.; Fuoco, D.; Elisei, F. Fast and Ultrafast Spectroscopic Investigation of Tetracycline Derivatives in Organic and Aqueous Media. *Phys. Chem. Chem. Phys.* **2010**, *12*, 15580−15591.

(9) Duarte, H. A.; Carvalho, S.; Paniago, E. B.; Simas, A. M. Importance of Tautomers in the Chemical Behavior of Tetracyclines. *J. Pharm. Sci.* **1999**, *88*, 111−120.

(10) Othersen, O. G.; Beierlein, F.; Lanig, H.; Clark, T. Conformations and Tautomers of Tetracycline. *J. Phys. Chem. B* **2003**, *107*, 13743−13749.

(11) Naidong, W.; Hua, S.; Roets, E.; Busson, R.; Hoogmartens, J. Investigation of Keto-Enol Tautomerism and Ionization of Doxycycline in Aqueous Solutions. *Int. J. Pharm. (Amsterdam, Neth.)* **1993**, *96*, 13−21.

(12) Stezowski, J. J. Chemical-Structural Properties of Tetracycline Derivatives. 1. Molecular Structure and Conformation of the Free Base Derivatives. *J. Am. Chem. Soc.* **1976**, *98*, 6012−6018.

(13) Lanig, H.; Gottschalk, M.; Schneider, S.; Clark, T. Conformational Analysis of Tetracycline using Molecular Mechanical and Semiempirical MO-Calculations. *J. Mol. Model.* **1999**, *5*, 46−62.

(14) Dos Santos, H. F.; Nascimento, C. S., Jr.; Belletato, P.; De Almeida, W. B. The Conformational and Tautomeric Equilibrium of 5a,6-Anhydrotetracycline in Aqueous Solution at pH 7. *J. Mol. Struct.: THEOCHEM* **2003**, *626*, 305−319.

(15) Schmitt, M. O.; Schneider, S. Spectroscopic Investigation of Complexation between Various Tetracyclines and Mg^{2+} or Ca^{2+}. *PhysChemComm* **2000**, *3*, 42−55.

(16) Schneider, S.; Brehm, G.; Schmitt, M.; Leypold, C.; Matousek, P.; Towrie, M. Picosecond Time Resolved Fluorescence of Tetracycline and its Complexes with Mg^{2+} or Ca^{2+}, Lasers for Science Facility Programme—Chemistry Central Laser Facility Annual Report, 2001/2002.

(17) Schneider, S.; Schmitt, M. O.; Brehm, G.; Reiher, M.; Matousek, P.; Towrie, M. Fluorescence Kinetics of Aqueous Solutions of Tetracycline and its Complexes with Mg^{2+} and Ca^{2+}. *Photochem. Photobiol. Sci.* **2003**, *2*, 1107−1117.

(18) Carlotti, B.; Cesaretti, A.; Elisei, F. Complexes of Tetracyclines with Divalent Metal Cations Investigated by Stationary and Femtosecond-Pulsed Techniques. *Phys. Chem. Chem. Phys.* **2012**, *14*, 823−834.

(19) Cesaretti, A.; Carlotti, B.; Clementi, C.; Germani, R.; Elisei, F. Effect of Micellar and Sol−Gel Media on the Spectral and Kinetic Properties of Tetracycline and its Complexes with Mg^{2+}. *Photochem. Photobiol. Sci.* **2014**, *13*, 509−520.

(20) Nishiyama, N.; Bae, Y.; Miyata, K.; Fukushima, S.; Kataoka, K. Smart Polymeric Micelles for Gene and Drug Delivery. *Drug Discovery Today* **2005**, *2*, 21−26.

(21) Gupta, P.; Vermani, K.; Garg, S. Hydrogels: from Controlled Release to pH-Responsive Drug Delivery. *Drug Discovery Today* **2002**, *7*, 569−579.

(22) Schmaljohann, D. Thermo- and pH-Responsive Polymers in Drug Delivery. *Adv. Drug Delivery Rev.* **2006**, *58*, 1655−1670.

(23) Bae, Y.; Jang, W. D.; Nishiyama, N.; Fukushima, S.; Kataoka, K. Multifunctional Polymeric Micelles with Folate-Mediated Cancer Cell Targeting and pH-Triggered Drug Releasing Properties for Active Intracellular Drug Delivery. *Mol. BioSyst.* **2005**, *1*, 242−250.

(24) Chen, W.; Meng, F.; Cheng, R.; Zhong, Z. pH-Sensitive Degradable Polymersomes for Triggered Release of Anticancer Drugs: A Comparative Study with Micelles. *J. Controlled Release* **2010**, *142*, 40−46.

(25) Sawant, R. M.; Hurley, J. P.; Salmaso, S.; Kale, A.; Tolcheva, E.; Levchenko, T. S.; Torchilin, V. P. "SMART" Drug Delivery Systems: Double-Targeted pH-Responsive Pharmaceutical Nanocarriers. *Bioconjugate Chem.* **2006**, *17*, 943−949.

(26) Hruby, M.; Konak, C.; Ulbrich, K. Polymeric Micellar pH-Sensitive Drug Delivery System for Doxorubicin. *J. Controlled Release* **2005**, *103*, 137−148.
(27) Brinchi, L.; Germani, R.; Di Profio, P.; Marte, L.; Savelli, G.; Oda, R.; Berti, D. Viscoelastic Solutions Formed by Worm-like Micelles of Amine Oxide Surfactant. *J. Colloid Interface Sci.* **2010**, *346*, 100−106.
(28) Goracci, L.; Germani, R.; Rathman, J. F.; Savelli, G. Anomalous Behavior of Amine Oxide Surfactants at the Air/Water Interface. *Langmuir* **2007**, *23*, 10525−10532.
(29) Bartocci, G.; Masetti, F.; Mazzucato, U.; Spalletti, A.; Baraldi, I.; Momicchioli, F. Photophysical and Theoretical Studies of Photo-isomerism and Rotamerism of trans-Styrylphenanthrenes. *J. Phys. Chem.* **1987**, *91*, 4733−4743.
(30) Carlotti, B.; Flamini, R.; Spalletti, A.; Marrocchi, A.; Elisei, F. Comprehensive Photophysical Behaviour of Ethynyl Fluorenes and Ethynyl Anthracenes Investigated by Fast and Ultrafast Time-Resolved Spectroscopy. *ChemPhysChem* **2012**, *13*, 724−735.
(31) Barbafina, A.; Latterini, L.; Carlotti, B.; Elisei, F. Characterization of Excited States of Quinones and Identification of their Deactivation Pathways. *J. Phys. Chem. A* **2010**, *114*, 5980−5984.
(32) Barbafina, A.; Amelia, M.; Latterini, L.; Aloisi, G. G.; Elisei, F. Photophysical Properties of Quinolizinium Salts and Their Interactions with DNA in Aqueous Solution. *J. Phys. Chem. A* **2009**, *113*, 14514−14520.
(33) Pizzoli, G.; Lobello, M. G.; Carlotti, B.; Elisei, F.; Nazeeruddin, M. K.; Vitillaro, G.; De Angelis, F. Acid−Base Properties of the N3 Ruthenium(II) Solar Cell Sensitizer: a Combined Experimental and Computational Analysis. *Dalton Trans.* **2012**, *41*, 11841−11848.
(34) Garcia-Rio, L.; Herves, P.; Mejuto, J. C.; Parajo, M.; Perez-Juste, J. Association Constant of Crystal Violet in Micellar Aggregates: Determination by Spectroscopic Techniques. *J. Chem. Res.* **1998**, 716−717.
(35) Costas-Costas, U.; Bravo-Diaz, C.; Gonzalez-Romero, E. Sodium Dodecyl Sulfate Micellar Effects on the Reaction between Arenediazonium Ions and Ascorbic Acid Derivatives. *Langmuir* **2003**, *19*, 5197−5203.
(36) Melik-Nubarov, N. S.; Kozlov, M. Y. Evaluation of Partition Coefficients of Low Molecular Weight Solutes between Water and Micelles of Block Copolymer of Ethylene Oxide Based on Dialysis Kinetics and Fluorescence Spectroscopy. *Colloid Polym. Sci.* **1998**, *276*, 381−387.
(37) van Stokkum, I. H. M.; Larsen, D. S.; van Grondelle, R. Global and Target Analysis of Time-Resolved Spectra. *Biochim. Biophys. Acta* **2004**, *1657*, 82−104.
(38) Snellenburg, J. J.; Laptenok, S. P.; Seger, R.; Mullen, K. M.; van Stokkum, I. H. M. Glotaran: A Java-Based Graphical User Interface for the R Package TIMP. *J. Stat. Software* **2012**, *49*, 1−22.
(39) Steinbach, P. J.; Ionescu, R.; Matthews, C. R. Analysis of Kinetics using a Hybrid Maximum-Entropy/Nonlinear-Least-Squares Method: Application to Protein Folding. *Biophys. J.* **2002**, *82*, 2244−2255.
(40) Steinbach, P. J. Inferring Lifetime Distributions from Kinetics by Maximizing Entropy using a Bootstrapped Model. *J. Chem. Inf. Comput. Sci.* **2002**, *42*, 1476−1478.
(41) Stephen, C. R.; Murai, K.; Burning, K. J.; Woodward, R. B. Acidity Constants of the Tetracycline Antibiotics. *J. Am. Chem. Soc.* **1956**, *78*, 4155−4158.
(42) Newton, D.; Kluza, R. pKa Values of Medicinal Compounds in Pharmacy Practice. *Drug Intell. Clin. Pharm.* **1978**, *12*, 546−554.
(43) Costantino, F.; Gentili, P. L.; Audebrand, N. A New Dual Luminescent Pillared Cerium(IV)sulfate−diphosphonate. *Inorg. Chem. Commun.* **2009**, *12*, 406−408.
(44) Gentili, P. L.; Clementi, C.; Romani, A. Ultraviolet−Visible Absorption and Luminescence Properties of Quinacridone−Barium Sulfate Solid Mixtures. *Appl. Spectrosc.* **2010**, *64*, 923−929.
(45) Di Nunzio, M. R.; Gentili, P. L.; Romani, A.; Favaro, G. Role of the Microenvironment on the Fluorescent Properties of a Spirooxazine. *Chem. Phys. Lett.* **2010**, *491*, 80−85.
(46) Di Nunzio, M. R.; Gentili, P. L.; Romani, A.; Favaro, G. Photochromism and Thermochromism of some Spirooxazines and Naphthopyrans in the Solid State and in Polymeric Film. *J. Phys. Chem. C* **2010**, *114*, 6123−6131.
(47) Penconi, M.; Gentili, P. L.; Massaro, G.; Elisei, F.; Ortica, F. A Triplet−Triplet Annihilation Based Up-Conversion Process Investigated in Homogeneous Solutions and Oil-in-Water Microemulsions of a Surfactant. *Photochem. Photobiol. Sci.* **2014**, *13*, 48−61.
(48) Siemiarczuk, A.; Ware, W. R. Pyrene Lifetime Broadening in SDS Micelles. *Chem. Phys. Lett.* **1990**, *167*, 263−268.
(49) Brown, W.; Rymden, R.; van Stam, J.; Almgren, M.; Svensk, G. Static and Dynamic Properties of Nonionic Amphiphile Micelles: Triton X-100 in Aqueous Solution. *J. Phys. Chem.* **1989**, *93*, 2512−2519.
(50) Gentili, P. L.; Ortica, F.; Favaro, G. Static and Dynamic Interaction of a Naturally Occurring Photochromic Molecule with Bovine Serum Albumin Studied by UV−Visible Absorption and Fluorescence Spectroscopy. *J. Phys. Chem. B* **2008**, *112*, 16793−16801.
(51) Alcala, J. R.; Gratton, E.; Prendergast, F. G. Interpretation of Fluorescence Decays in Proteins using Continuous Lifetime Distributions. *Biophys. J.* **1987**, *51*, 925−936.
(52) Kumar, A. T.; Zhu, L.; Christian, J. F.; Demidov, A. A.; Champion, P. M. On the Rate Distribution Analysis of Kinetic Data using the Maximum Entropy Method: Applications to Myoglobin Relaxation on the Nanosecond and Femtosecond Timescales. *J. Phys. Chem. B* **2001**, *105*, 7847−7856.
(53) Jimenez, R.; Fleming, G. R.; Kuman, P. V.; Maroncelli, M. Femtosecond Solvation Dynamics of Water. *Nature* **1994**, *369*, 471−473.
(54) Horng, M. L.; Gardecki, J. A.; Papazyan, A.; Maroncelli, M. Subpicosecond Measurements of Polar Solvation Dynamics: Coumarin 153 Revisited. *J. Phys. Chem.* **1995**, *99*, 17311−17337.
(55) Pal, S. K.; Sukul, D.; Mandal, D.; Sen, S.; Bhattacharyya, K. Solvation Dynamics of DCM in Micelles. *Chem. Phys. Lett.* **2000**, *327*, 91−96.
(56) De, D.; Datta, A. Modulation of Ground- and Excited-State Dynamics of [2,2′-Bipyridyl]-3,3′-diol by Micelles. *J. Phys. Chem. B* **2011**, *115*, 1032−1037.
(57) Ghatak, C.; Rao, V. G.; Mandal, S.; Ghosh, S.; Sarkar, N. An Understanding of the Modulation of Photophysical Properties of Curcumin inside a Micelle Formed by an Ionic Liquid: A New Possibility of Tunable Drug Delivery System. *J. Phys. Chem. B* **2012**, *116*, 3369−3379.
(58) Gentili, P. L. Small Steps towards the Development of Chemical Artificial Intelligent Systems. *RSC Adv.* **2013**, *3*, 25523−25549.